Mine Water and the Environment (2021) 40:426–432
https://doi.org/10.1007/s10230-020-00749-9

TECHNICAL ARTICLE

# Model-based Seismic Imaging and Analysis of Karst Water Hazards in Coal Mining

**Xianxu Zhang**[1]

Received: 2 July 2019 / Accepted: 17 December 2020 / Published online: 19 January 2021


## Abstract

Accurate detection of karst water is the premise of karst water disaster control in coal mines. It is difficult to identify karst geological characteristics based on seismic data, so to solve this problem, a digital model including the coal measure strata and complete karst system was established based on the karst status of a coal mine in the Huaibei area of China. The entire process of seismic acquisition, processing, and interpretation was simulated and then the model was restored according to the seismic interpretation. Based on the results, karst identification and water inrush risk prediction were tried. The results allowed the overall karst geological framework, karst cave system, and stratum contact relationships to be restored more truly. Thus, seismic data can provide accurate geological information for large-scale hydrogeological mine exploration.

**Keywords** Coalfield · Karst seismic characteristics · Seismic simulation · Huaibei, China

## Introduction

China is the largest coal mining country in the world and karst water is a major water hazard problem there (Wu 2014; Xu et al. 2019). Karst water inrushes are very destructive and cause serious loss of property and lives (Hu and Tian 2010; Wu and Zhu 2004; Wu et al. 2013). Therefore it is necessary to carry out hydrogeological investigation in mines with karst water risks, to determine the position, spatial distribution, water yield property, recharge conditions, and contact relation of the water source, so as to provide basic data for mine inflow assessment and feasibility of mining by dewatering and depressurization (Jin et al. 2009; Li et al. 2018; Sun et al. 2016; Wu and Chen 2008). The thickness, distribution, stability, and constitutive relationship of different aquifer lithologies must be characterized for accurate aquifer reinforcement and reconstruction, to allow coal mining to safely succeed despite high hydrostatic pressure (Li et al. 2019; Ma 2005). Accurate detection of concealed water-flowing structures, faults, collapse columns, and faulted/fractured zones is also necessary since these can connect coal seams and aquifers (Wang et al. 2016; Wu et al. 2013, 2014).

Geophysical technologies are an important component of hydrogeological exploration. Among them, seismic techniques have been applied in China's coal mines for about 60 years, from initial exploration of resources to exploration for safe production (Dong 2007). However, seismic exploration is mainly used for structural understanding and less for karst water hazard exploration. This is because the scale of karstic development is relatively large, usually spanning an entire coal basin, while coal mine seismic exploration requirements are less than 10 $km^2$. In addition, seismic data uses the impedance difference between rocks or fluids for imaging and does not directly detect water. Thus, for hydrogeologists, seismic data is difficult to use effectively. Therefore, we established a geological model based on half a basin to simulate typical karst features and the contact relationship between karst and coal seam. Through numerical simulation, a seismic section corresponding to the model was obtained, which intuitively showed the response of karst landforms in seismic data, which helped hydrogeologists better understand the relationship between the geology and seismic data, and use seismic data for hydrogeological analysis.

✉ Xianxu Zhang
zhangxianxu@cctegxian.com

[1] Xi'an Research Institute of China Coal Technology and Engineering Group, Xi'an 710077, Shaanxi, China

## Karst Geological Characteristics and Geological Model

The karst development process is mainly influenced by ancient landforms. As shown in the karst environmental geological model (Fig. 1), karst landforms are generally divided into platforms, slopes and basins (James and Choquette 1988; Wu 2003). Mechanical corrosion of carbonate rock, such as dissolution, washout, subsurface erosion, and collapse, are typical geological products of karst landforms under hydrodynamic action. The most representative products are:

(1) Plane of unconformity: this sign of karst development indicates a time of crustal uplift or lowering of sea level, which exposed the protolith above the water level and subjected it to weathering and denudation. Landforms such as rivers, gullies, and karst caves are developed, so the plane of unconformity is commonly rough and uneven.
(2) Karst caves: in areas with sufficient water supply and strong hydrodynamic force, vertical seepage tends to dominate, and vertical karst caves develop. In areas below the phreatic surface or with weak hydrodynamic force, horizontal runoff dominates, and horizontal karst caves develop. The two types of karst caves combine to form a crisscross underground water system. Over time, the caves are gradually filled with loose sediments, and some collapse, forming collapse columns.

## Karst Numerical Model

Using digital models to simulate typical karst geological bodies, we can intuitively analyze the response of typical karst geological bodies, including unconformity plane, vertical and horizontal karst caves, and collapse columns in seismic data, clarify the shape of typical karst geological bodies, and enable geologists to better use seismic data for geological interpretation.

### Model Design

A model was developed (Fig. 2) based on James' geological model and the geological conditions of the Huaibei coalfield in China. In the model, the limestone strata are directly covered by coal measures strata and these strata contain a 10 m thick coal seam; the coal measure strata are covered by relatively low velocity and density material to simulate the Quaternary strata. The coal measures and Quaternary strata present an angular unconformity contact relationship, and a 100 m fault was incorporated in the coal measures and limestone strata to simulate transformation of the structure by later geological movement (Fig. 2). The petrophysical parameters of the model are shown in Table 1. The

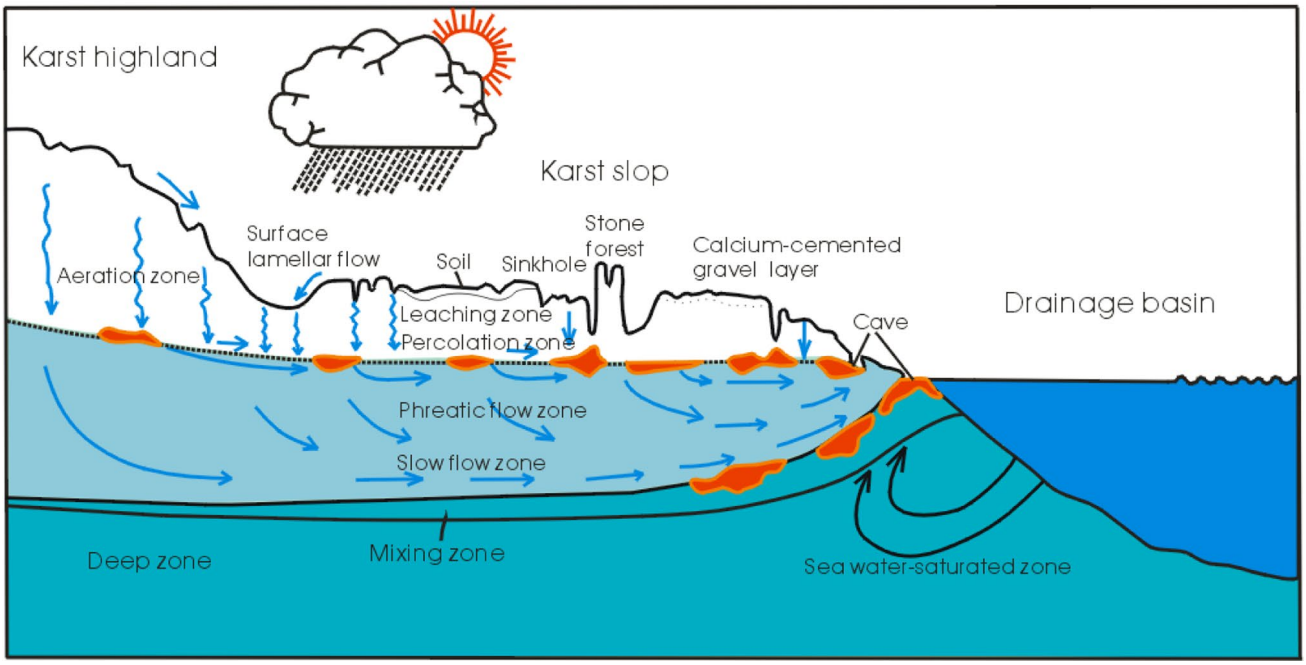


**Fig. 1** Karst environmental geological model (James 1988)

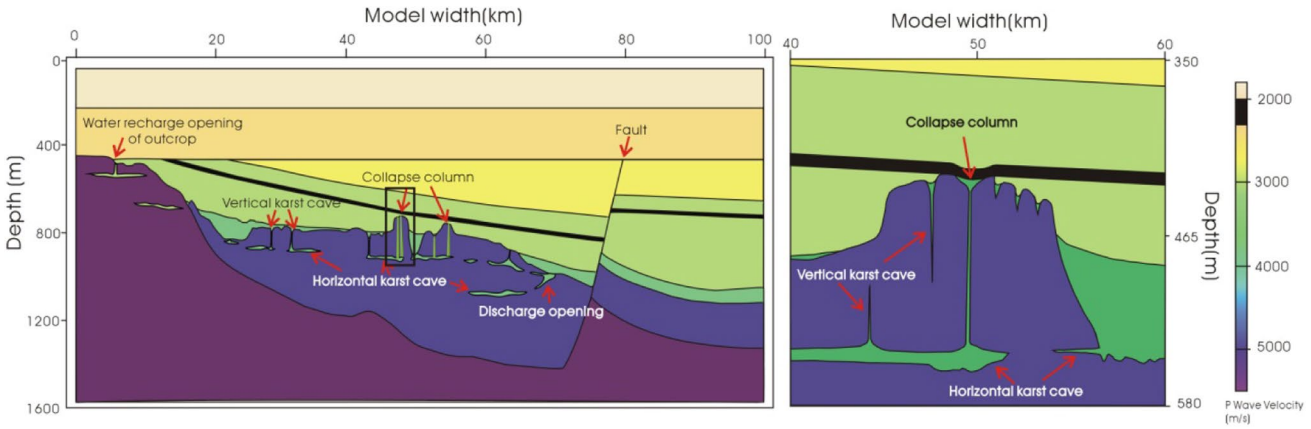


**Fig. 2** Digital models of coal measures and Ordovician limestone

**Table 1** Physical parameters of model

| No. | Lithology | Velocity of P wave, m/s | Density, g/cc |
|---|---|---|---|
| 1 | Loess, sand, mudstone | 1800 | 1.20 |
| 2 | Sand, mudstone | 2500 | 2.20 |
| 3 | Sand, mudstone | 3000 | 2.20 |
| 4 | Sandstone, siltstone, mudstone | 3300 | 2.25 |
| 5 | Coal | 2200 | 1.60 |
| 6 | Sandstone, siltstone, mudstone | 3300 | 2.25 |
| 7 | Karst remains | 4000 | 2.35 |
| 8 | Limestone | 5000 | 2.50 |
| 9 | Limestone | 5500 | 2.57 |

parameters are from the literature (Li et al. 2011; Mavko et al. 1998; Zhu et al. 2008) and logging data from the Huaibei area.

To simulate a complete karst system, the model was designed to be 100 km wide and 1600 m deep. Nine layers were included in the model; the parameters are shown in Table 1. Layers 1–2 simulated horizontal sandstone and mudstone strata from the Quaternary.

Layers 3–6 simulated Jurassic to Carboniferous strata: the major component of layer 6 was quickly deposited sandstone and siltstone of greatly varied thickness (0–100 m); the terrain is filled with sediments. Layer 5 was basically monoclinal coal seams, averaging 10 m thick. Layer 4 is the coal seam roof, averaging about 40 m; its major components were mudstone, sandstone, and siltstone. A normal fault was developed in the Carboniferous strata, breaking layers 3–9, with a displacement of about 100 m.

Layer 7 simulated the Carboniferous Benxi strata, mainly siltstone and alumina (residual sediments eroded up-gradient and deposited here). Layer 8 simulated Middle Ordovician strata, of which the limestone was highly denuded, with very developed karst. Its degree of denudation was related to the relief, decreasing less at lower paleo-terrain elevations. The strata on the paleo-platform were completely denuded, the strata on the slope were slightly denuded, while the strata in the basin were well preserved. Simulating the real world, the plane of unconformity was designed to be the top karst interface, with rolls and swells due to denudation; there were karst monadnocks on the karst slope. The karst forms were predominantly sinkholes in the karst highland, a combination of vertical and horizontal caves on the slope, and predominantly horizontal caves and caved-in collapse columns at the center of the basin.

The lowest layer simulated the Lower Ordovician strata; the rock was limestone with non-developed karst and a small degree of denudation, such that the paleo-landform was largely preserved. From left to right, it was bench terrace, slope, and basin.

## Model Simulation

The model used Tesseral 2D (version 6.3.2) software and the acoustic wave equation method for numerical simulation. Based on the calculation time and accuracy, the model was divided into 2.5 m × 2.5 m grid size. The actual seismic exploration method was simulated, using a shooting process to obtain the raw shots data; data processing was performed on the raw shots to obtain the seismic section of the model.

The model incorporated 980 shots in the middle array. The array moved with rolling reception following the shot position, with 200 receivers spaced 10 m apart. The dominant frequency of the wavelet was 60 Hz; its coverage was tenfold with a sampling interval of 1 ms. The model raw shot data are shown in Fig. 3.

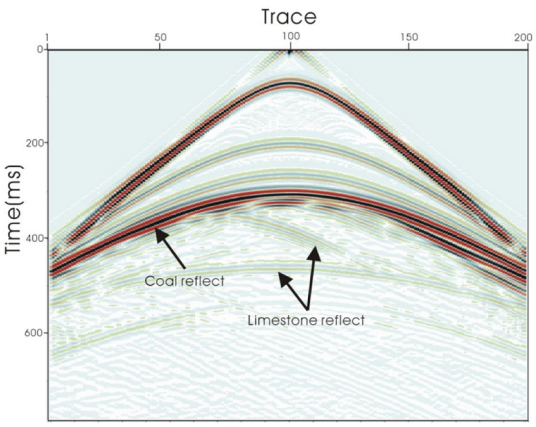


**Fig. 3** Raw shot data

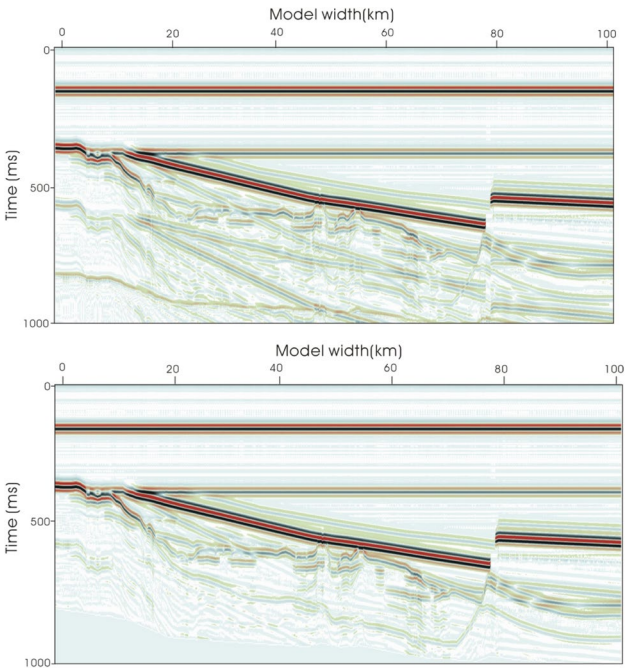


**Fig. 4** Before (**a**) and after (**b**) multiple suppression

## Model Data Processing and Interpretation

### Data Processing

Since there was no noise in the model data, and the model's structure and the velocity of the strata were known, data processing was relatively simple; GeoEast 3.3.2 software was used to process and interpret the data. Preliminary processing results are shown in Fig. 4a, which shows that the data processing had some peculiarities, particularly: (1) The coal seam has a shielding effect on seismic waves, weakening the reflected energy of the underlying strata and making it difficult to identify; (2) The multiple energy waves developed in the Quaternary strata and coal seams was also very strong, which seriously affected the imaging of the strata below the coal seam (Fig. 4a).

For the shielding problem, the known energy suppression factor of the coal seam was used to address the weak reflected energy of the underlying strata. Based on the known premise of the model, a multiple development reflection layer was selected, and the multiple was suppressed using the prediction elimination method in a split window. The result is shown in Fig. 4b.

### Data Interpretation and Analysis

From the imaging profiles (Fig. 5), the whole stratigraphic framework was consistent with the model's design, and the reflection delineated the stratigraphic sequence. Because reflected energy is determined by the wave impedance difference of rocks, so the reflection from coal seams was the strongest, followed by the bottom of the Quaternary. The strata with the strongest reflection below the coal seams was the weathered crust at the top limestone interface, and the reflection from inside the Ordovician limestone was the weakest. The reflections from horizontal karst caves was stronger but its transverse continuity was poor. The reflected energy from the reflecting interface of two sets of limestone was weaker but had better continuity.

The structural form of the reflections of the Quaternary interfaces was horizontal, and the structures of the coal seams clearly appeared as monoclines. The undulations of the reflecting interface of the weathered crust correctly reflected its geological form. Imaging of vertical karst caves was difficult due to their geological structure, while the reflections from horizontal karst caves was stronger but discontinuous. Inside the Ordovician, the interface of the two limestone sets delineated the sedimentary platforms, slope, and basin. Faults were expressed very clearly, allowing the correct position of the faults to be delineated.

The typical feature of a single coal seam was two wave peaks intercalated with a wave trough. Due to the strong reflection of the coal seams, the internal reflection of the coal measures strata was relatively weak, and easily disguised by the coal seam.

The Quaternary had horizontal reflections. Because of its weak digenesis and compaction, the compaction curves changed quickly, the impedance contrast was relatively large, and the reflections were relatively strong. Generally, the top interface of the Ordovician limestone was a weathered denuded plane because the limestone was easily eroded. In areas of flat paleo-landforms, the reflection event was relatively straight, while in areas with undulating paleo-landforms, the reflection was uneven. Because of the existence

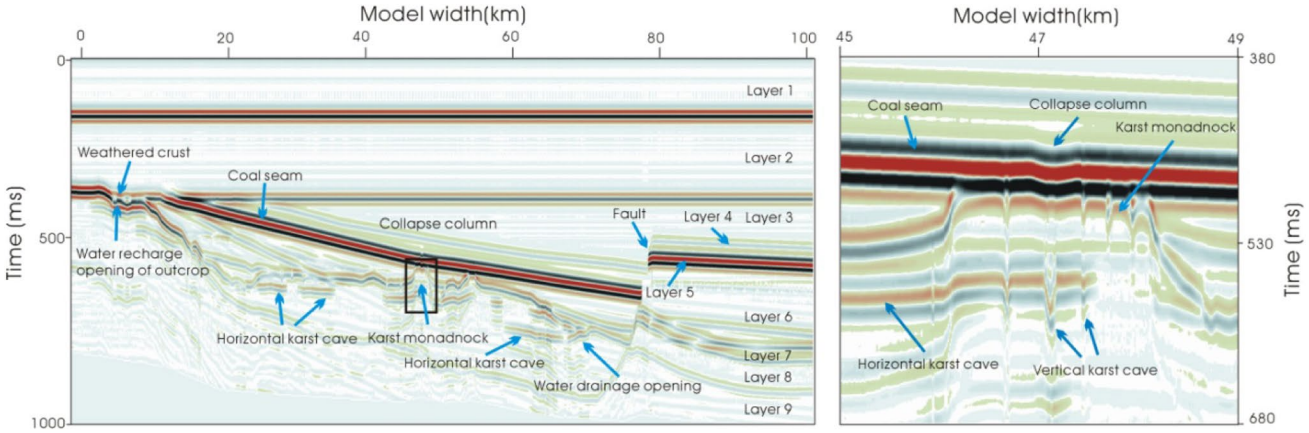


**Fig. 5** Interpretation of the model seismic section

of residual deposits, the reflected energy of weathered crust was generally stronger, but with overlying coal seams, its reflected energy will be weakened substantially.

Small geological bodies such as karst caves inside the limestone generally appeared as point and segment amplitude anomalies in seismic sections and linear or circular amplitude anomalies in horizontal slices. According to the model image (Fig. 5), different types of karst caves have different reflection patterns, mainly:

a. Horizontal karst caves had relatively strong reflections, and were easy to discriminate, particularly the large-scale caves and the large wave impedance contrast of filling materials. However, it was still much weaker than the reflection of coal seams and the top limestone interface. The difficulty of horizontal karst cave identification is related to the size and the observation direction of the survey line.
b. Reflections from vertical sinkholes were difficult to recognize because only the top of vertical sinkholes can be observed from the ground surface, while the top width of vertical sinkholes only ranged from 1 to 5 m. In addition, the reflected energy was very weak and difficult to recognize. However, strata thinned at the entrance of these vertical sinkholes, so that the landform basically appeared as a funnel, bending or weakening the reflection. The features could be used to identify vertical sinkholes.
c. Collapse columns proved similar to vertical karst caves, but more complex. Generally the diameter of collapse columns was larger than that of vertical sinkholes, so the seismic reflection from the top was relatively obvious, and collapse columns appeared as bead-like reflections.

In the models, the faults developed before the Quaternary formed. Because the fault throw was bigger, faults showed as disconnected reflections, which was particularly evident in the coal seams. At greater depths, because the dip of the faults was less, the fault plan also had a reflection.

### Geological Restoration

For hydrogeologists, seismic data is obscure and difficult to effectively use. Therefore, it is very important that seismic interpreters convert the horizons, faults and, geological bodies interpreted in the seismic sections into geological sections, which provides data for geological and hydrogeological analysis (Fig. 6).

It should be noted that since the seismic data is time domain data, the depth section can be obtained by time-depth conversion according to the velocity. Since the velocity of the model was known, the model could be better restored after time-depth conversion. The resolution of seismic data is limited, so it is difficult to distinguish geological bodies less than a quarter of the wavelength.

## Analysis of Water Inrush

According to the restored geological profile, the geometry and contact relationship of geological structures and karst bodies can be directly reflected, and the whole karst system can be clearly displayed, permitting hydrogeological analysis.

### Water-filling Space

Given the great amount of karst caves and fractures, there was a large amount of water-filled space. Because the thickness of the model's layer 6 between the coal seams and the limestone changed quickly, at place where the layer was thin, the capacity of confined water was weaker. Therefore, the

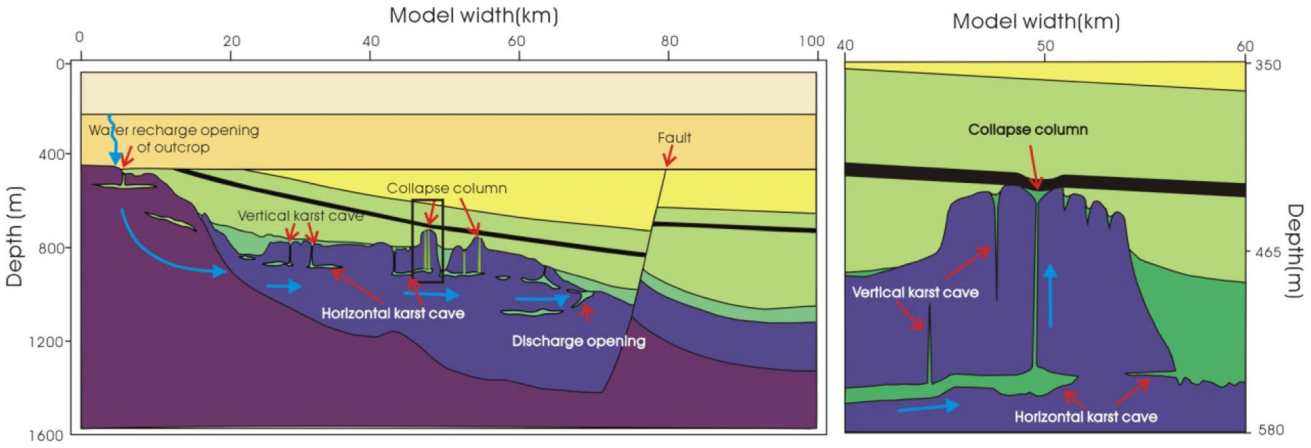


**Fig. 6** Geological profile

Ordovician limestone water constituted a serious threat for coal mining.

### Recharge of Ordovician Limestone Water Source

At places of unconformity, Ordovician are directly recharged by Quaternary groundwater. In addition, faults and associated fractured zones may be good water-flowing channels to recharge water to the limestone.

### Analysis of Water Inrush Risk

The layers separating the coal seams and limestone were layers 6 and 7, but because layer 7 was locally developed, the thickness of that layer 6 decided the water-isolating and pressure-resisting capacity. At coal outcrops, where coal seams unconformable contacted the sandstone of Quaternary, there was no water-isolating capacity, and the water inrush risk was high. On the model's left side, strata thinned: the aquiclude was 10 m thick, but had collapse columns, which meant that its water-isolating capacity was poor, and the water inrush risk was high. The minimum thickness of the aquiclude on the right side was 20 m and vertical karst caves were developed, which meant that water inrush risk was higher; where faults connected the coal seams and the limestone, water-isolating capacity was poor, and the inrush risk was high.

## Conclusion

Based on the geological conditions of coal fields in Huaibei area of China and typical karst environmental geological theory, we established a 100 km model that simulates the entire karst system of the coal-bearing basin. Data processing, interpretation, geological restoration, and hydrogeological analysis were carried out, after processing and interpretation of the modeled seismic data, it was clear that the seismic data was directly related to the properties of the rock, and can be converted into a geological profile that can be used by hydrologists for hydrogeological analysis.

In reality, the seismic exploration area of coal mines is too small, making it difficult to identify karst and summarize the laws of karst geology in locally observed data. In this paper, the model was used as a bridge to simulate the whole karst system, and typical seismic facies such as the coal seam, Ordovician limestone top reflection, and karst cave reflection in the coal-bearing basin were summarized. According to the model results, identification of vertical karst caves is more difficult than horizontal caves, but we can use an identified horizontal cave and the sedimentary law to improve the success rate of identifying vertical karst caves.

**Acknowledgements** This work was supported by the National Key R&D Program of China 2018YFC0807804.

## References

Dong SN (2007) Status and outlook of geological guarantee technology for safe and efficient production in coal mines. Coal Sci Technol 35(3):1–5 **(Chinese)**

Hu WY, Tian G (2010) Types and prevention and control countermeasures of coal mine water hazards in China. Coal Sci Technol 38(1):92–96 **(Chinese)**

James NP, Choquette PW (1988) Paleokarst. Springer, Berlin

Jin DW, Liu Q, Wang L, Ding X (2009) Status and outlook of research on coal mine (deposit) hydrogeology. Coal Geol Explor 37(5):28–36 **(Chinese)**

Li YF, Cheng JY, Xiong XJ et al (2011) 3D seismic forward modeling of collapse column and comparison. J China Coal Soc 36(3):456–460 **(Chinese)**

Li B, Wu Q, Duan XQ, Chen MY (2018) Risk analysis model of water inrush through the seam floor based on set pair analysis. Mine Water Environ 37(2):281–287

Li H, Bai H, Wu J, Meng QB, Ma K (2019) a set of methods to predict water inrush from an Ordovician karst aquifer: a case study from the Chengzhuang mine. China Mine Water Environ 38(1):39–48

Ma PZ (2005) Water inrush discrimination model and water control countermeasures for under-pressure mining of lower coal seams in north China coalfields. J China Coal Soc 30(5):608–612 **(Chinese)**

Mavko G, Mukerji T, Dvorikin J (1998) The rock physics handbook: tools for seismic analysis in porous media. Cambridge University, London

Sun WJ, Zhou WF, Jiao J (2016) Hydrogeological classification and water inrush accidents in China's coal mines. Mine Water Environ 35(2):214–220

Wang CS, Wu Q, Ma HP et al (2016) Classification of mine hydrogeological types with complicated conditions. J China Coal Soc 41(3):696–702 **(Chinese)**

Wu Q (2003) Study on classification of types of mine environmental geological problems in China. Hydrogeol Eng Geol 27(5):107–112 **(Chinese)**

Wu Q (2014) Progress, problems and outlook in research of prevention and control and resource utilization of mine water in China. J China Coal Soc 39(5):795–805 **(Chinese)**

Wu Q, Chen Q (2008) Study on environmental effect induced by mine environmental problems. Hydrogeol Eng Geol 5(1):81–85 **(Chinese)**

Wu Q, Zhu QJ (2004) Brief talk on some problems of groundwater geophysical exploration techniques. Hydrogeol Eng Geol 29(3):111–114 **(Chinese)**

Wu Q, Zhao SQ, Sun WJ (2013) Classification of China's coal mine hydrogeological types and analysis of their characteristics. J China Coal Soc 38(6):901–905 **(Chinese)**

Wu Q, Cui FP, Zhao SQ et al (2014) Analysis on type's characteristics of mine water hazard. J China Coal Soc 38(4):561–565 **(Chinese)**

Xu YC, Du MZ, Luo YQ (2019) Using water injection to prevent shaft failure in the Jining no. 3 coal mine, China. Mine Water Environ 38(1):60–71

Zhu GM, Li GH, Cheng JY (2008) Numerical simulation of seismic survey in coalmine roadway. J China Coal Soc 33(11):1263–1267 **(Chinese)**